Supportive Information

Ligand labilization gates intramolecular electron transfer in molecular photocatalyst

Louis Blechschmidt,[ab] Linda Zedler, [ab] Alexander K. Mengele,[c] Sven Rau[c], Benjamin Dietzek-Ivanšić [ab]

[a.] *Institute of Physical Chemistry, Friedrich Schiller University Jena, Helmholtzweg 4, 07743 Jena, Germany*
[b.] *Department Functional Interfaces, Leibniz Institute of Photonic Technology (IPHT), Albert-Einstein-Straße 9, 07745 Jena, Germany*
[c.] *Institute of Inorganic Chemistry I, Ulm University, Albert-Einstein-Allee 11, 89081 Ulm, Germany.*

Corresponding author: Benjamin.dietzek@leibniz-ipht.de

Experimental details

Time-Resolved Spectroscopy (TAS)

General considerations. Femtosecond (fs) transient absorption (TA) spectra were collected by a previously custom-built setup.[1] A regenerative Ti:sapphire amplifier (Astrella, Coherent, USA) is used for the fundamental laser, delivering pulses of 5 mJ pulse energy at 1 kHz pulse repetition rate and 800 nm. The pulses have a duration of 80 fs. The pump wavelength is centered using a TOPAS-C Lightconversion, also from Coherent. A white light supercontinuum generated by focusing a fraction of the fundamental in a CaF_2 plate is used to probe the samples in a wide spectral range (340 to 750 nm). The pump beam is delayed in time with respect to the probe beam by means of an optical delay line and the polarization between probe and pump is set at the magic angle (54.7°). For all the experiments the stability of samples was ensured by recording the UV/Vis absorption spectra (JASCO V-670 spectrometer) at room temperature before and after fs TA measurement.

The fs TA spectra were displayed after chirp correction. The fs TA data were processed and analyzed by a global multi-exponential fit, using the Python Package KiMoPack.[2] A temporal window around time-zero was excluded in order to avoid contributions of the coherent-artifact region to the data analysis. Furthermore, a spectral band of ca. 30 nm around the pump-wavelength is omitted from the data analysis due to pump-scatter in this spectral range.

Table S1: Experimental and fitting parameters for the different TA-experiments. *a)* For TBA-salt concentrations below 35 mM. *b)* For higher TBA-salt concentrations (150 mM and 300 mM). *c)* The beam profile at the sample position for the temperature-dependent TA could not be determined since the respective camera does not fit into the cryostate. *d)* The initial parameters were estimated following the literature.[3] *e)* When varying all finite compounds in the global fit of the temperature-dependent datasets τ_1 and τ_2 did not show a trend over the temperature, see Table S2. The values were therefore averaged and fixed to improve the fitting of the temperature-sensitive τ_3 value.

TA-Experiment TBA-salt concentration	Temperature dependent 0 mM	TBA-salt dependent Below 35 mM 150 & 300 mM
Cuvette pathlength	1 cm	1 mm
Excitation Wavelength (λ_{exc})	400 nm	490 nm
Steady state absorption at λ_{exc}	0.3 OD	0.35…0.5 OD[a] 0.3…0.4 OD[b]
Pump Power	0.8 mW	0.4 mW
Pump-beam diameter at sample position	-[c]	780 µm[a] 900 µm[b]
Omitted spectral band around λ_{exc}	387…420 nm	480…510 nm
Ignored time window around Δt = 0 ps	-1.5…+0.4 ps	-0.3…+0.3 ps
Initial global fit parameter-set[d]	τ_1 = 0.82 ps[e]; τ_2 = 7.9 ps[e]; τ_3 = 450 ps; τ_{inf} – only vary τ_3	τ_1 = 1 ps; τ_2 = 11 ps; τ_3 = 450 ps; τ_{inf} - vary all finite compounds

Temperature-dependent fs TA. Spectra were recorded by putting the sample in a 1 cm cuvette, specialized for cryostat experiments. The sample was purged with nitrogen gas for 10 min. Afterwards the cuvette was placed in a temperature-controlled cryostat (Optistat DN, Oxford Instrument) cooled with liquid nitrogen. Temperatures were set by an intelligent temperature controller (ITC 503S, Oxford Instruments) and the real-time temperature inside the cuvette was monitored by a temperature sensor (PT100, SensorShop24, Germany). All samples have been cooled down until stable before starting the pump-probe experiment.

Temperature dependent fs TA data of **RutpphRhCp***

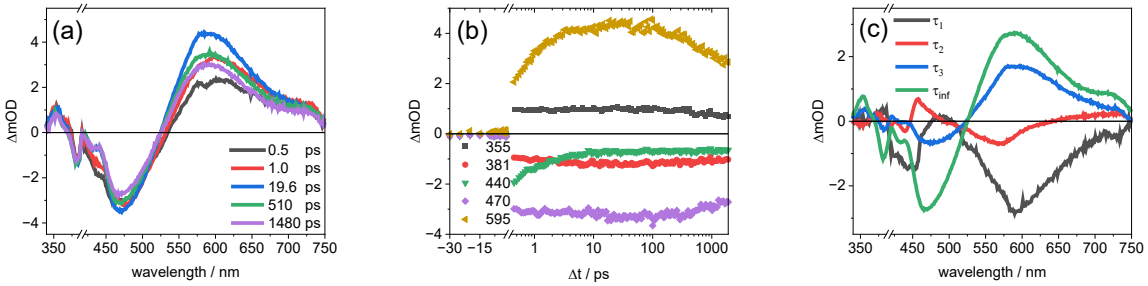

Figure S1: Chirp-corrected raw transient spectra (a), chirp-corrected raw kinetic traces (b) and decay associated spectra received from global fitting of RutpphzRhCp* dissolved in ACN, measured at 246 K in a standard 1 mm cuvette without the addition of further compounds.

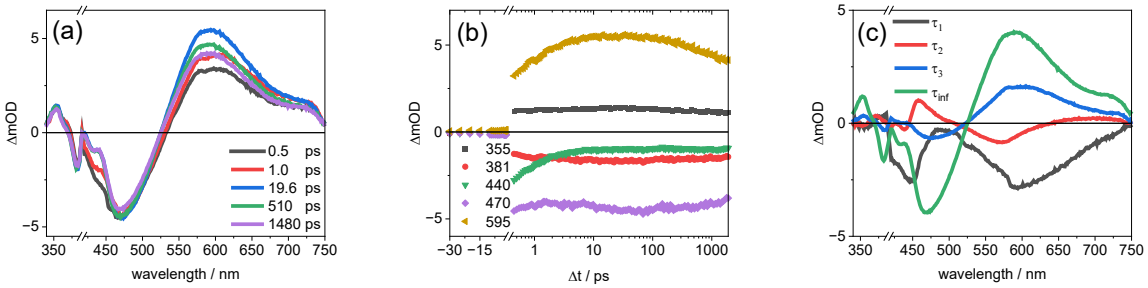

Figure S2: Chirp-corrected raw transient spectra (a), chirp-corrected raw kinetic traces (b) and decay associated spectra received from global fitting of RutpphzRhCp* dissolved in ACN, measured at 263 K in a standard 1 mm cuvette without the addition of further compounds.

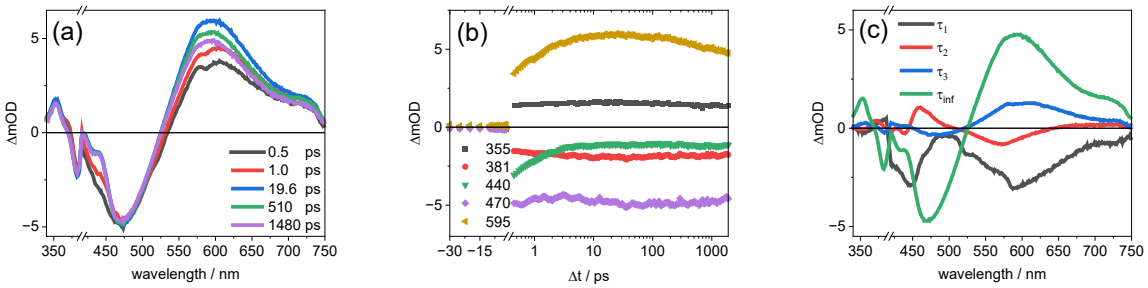

Figure S3: Chirp-corrected raw transient spectra (a), chirp-corrected raw kinetic traces (b) and decay associated spectra received from global fitting of RutpphzRhCp* dissolved in ACN, measured at 283 K in a standard 1 mm cuvette without the addition of further compounds.

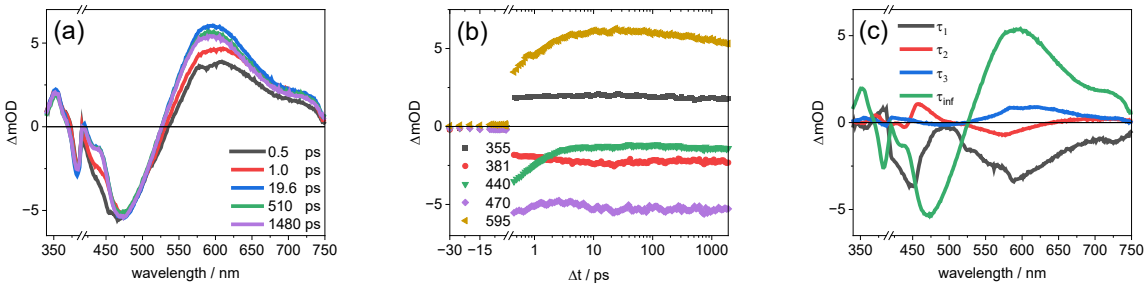

Figure S4: Chirp-corrected raw transient spectra (a), chirp-corrected raw kinetic traces (b) and decay associated spectra received from global fitting of RutpphzRhCp* dissolved in ACN, measured at 303 K in a standard 1 mm cuvette without the addition of further compounds.

Table S2: Fitting results of the time constants for each experiment if all compounds are free to vary in the fitting procedure. The fitted time constants of the three processes were on one hand compared across all values and in groups divided into four temperature areas (240 K, 260 K, 280 K and 300 K). The mean values and the respective mean deviation for the time constants are shown in brackets with the respective relative error below in parathesis.

T_{Sample} / K	τ_1 / ps	τ_2 / ps	τ_3 / ps
244.25	0.70	8.8	710
248.70	0.70 [0.73±0.04]	7.5 [8.6±0.7]	647 [861±243]
244.35	0.80 (6%)	9.5 (9%)	1225 (28%)
262.95	0.88	6.8	726
263.15	0.78 [0.83±0.03]	5.6 [7.4±1.6]	639 [699±40]
263.45	0.83 (4%)	9.9 (22%)	732 (6%)
282.50	0.76	4.3	500
283.00	0.85 [0.79±0.04]	6.5 [6.7±1.7]	582 [522±40]
283.00	0.77 (5%)	9.2 (25%)	484 (8%)
302.75	0.47	3.9	521
302.80	0.89 [0.80±0.06]	7.6 [7.1±0.7]	427 [477±33]
302.75	0.78 (7%)	9.7 (30%)	482 (7%)
Overall mean	[0.79±0.05] (6%)	7.4±1.7 (23%)	640±140 (22%)

Table S3: Thermic parameters and fitting results for the temperature-dependent TA experiments. For each temperature area (240 K, 260 K, 280 K, 300 K) three experiments were performed. The average sample temperature and the τ_3 values with their respective mean derivation were used for the further analysis via the Arrhenius-Plot in Figure 2. Furthermore, the table shows the ratio between the remaining offset and the maximum signal of the individual kinetics in the ESA region from 570 nm to 630 nm, summarized in Figure 1(b) in the main text as well as the time constant and offset for the monoexponentially fit of the normalized decay kinetics at 590 nm, starting after a delay-time of 10 ps. The corresponding kinetic graphs can be found in Figure S5.

Exp No.	Temperature	Global Fit	$\int_{570\,nm}^{630\,nm} TAS\, d\Delta t$	Exp Decay Fit 590 nm $I_{590nm}(\Delta t) = y_0 + A_1 e^{-\frac{x}{t_1}}$	
	T / K	τ_3 / ps	I_{fin}/I_{Max}	t_1	y_0
240 K – 1	244.25	737	0.623	809	0.600
240 K – 2	248.70	660	0.699	717	0.691
240 K – 3	244.35	1249	0.888	1283	0.849
240 K – mean	[245.45±1.96]	[882±245]	[0.737±0.101]	[936±231]	[0.713±0.090]
260 K – 1	262.95	703	0.742	830	0.712
260 K – 2	263.15	623	0.691	673	0.714
260 K – 3	263.45	752	0.864	777	0.868
260 K – mean	[263.18±0.18]	[693±46]	[0.766±0.066]	[760±58]	[0.765±0.069]
280 K – 1	283.00	564	0.791	672	0.791
280 K – 2	282.50	482	0.701	542	0.727
280 K – 3	283.00	506	0.878	470	0.874
280 K – mean	[282.83±0.22]	[517±31]	[0.790±0.059]	[561±74]	[0.797±0.051]
300 K – 1	302.75	487	0.847	675	0.842
300 K – 2	302.80	416	0.761	452	0.772
300 K – 3	302.75	493	0.871	487	0.881
300 K – mean	[302.77±0.02]	[465±33]	[0.826±0.044]	[538±91]	[0.832±0.040]

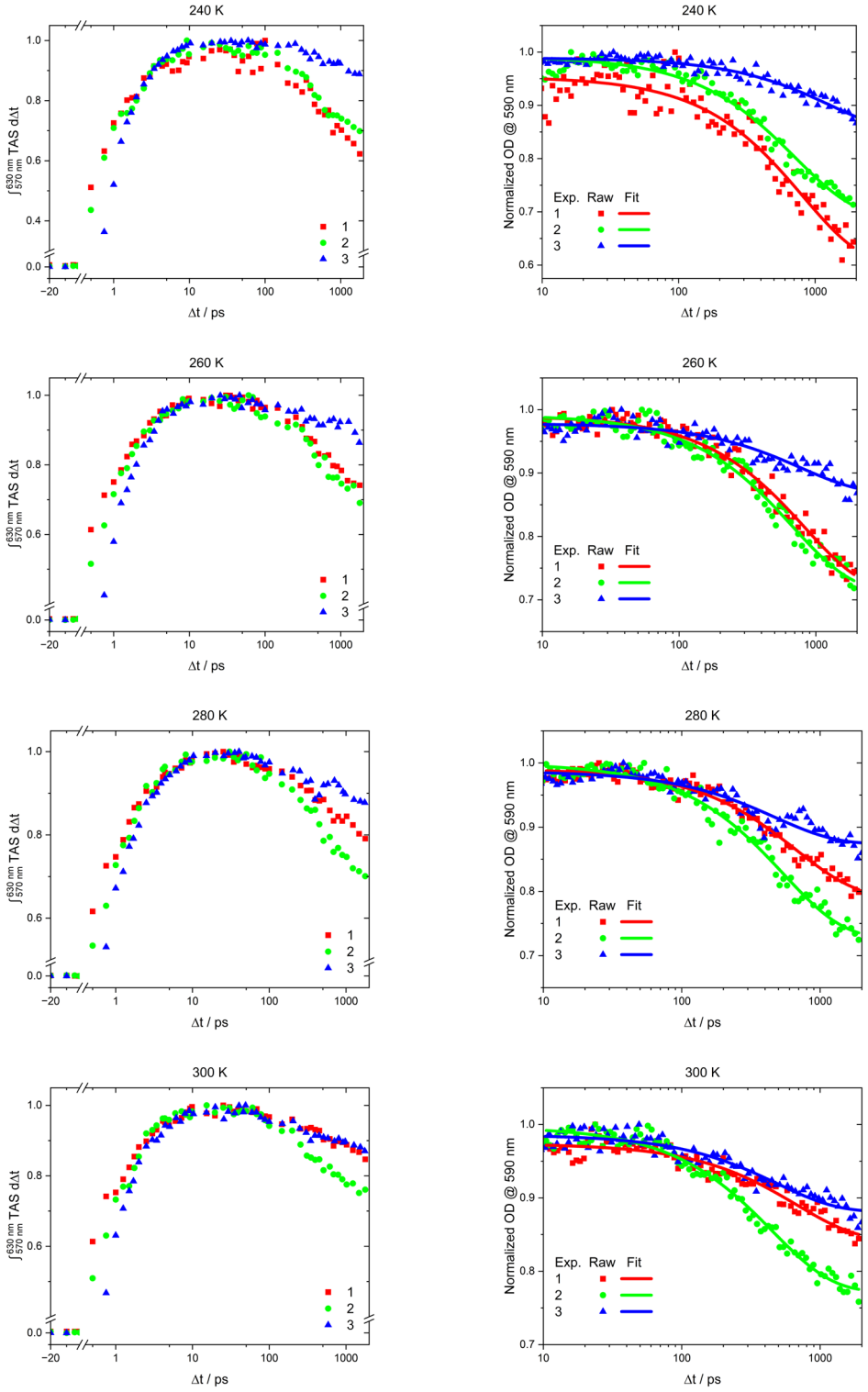

Figure S5: Integrated TAS over time in the spectral region from 570 nm to 630 nm (left) and raw kinetics at 590 nm together with the respective monoexponentially fits of the decaying branches (right). Each graph consists of the results from the three experiments per temperature area (from top to bottom: 240 K, 260 K, 280 K and 300 K). See Table S3 for key values related to these graphs.

TBA-salt dependent fs TA data of **RutpphzRhCp***

Pure RutpphzRhCp* in ACN

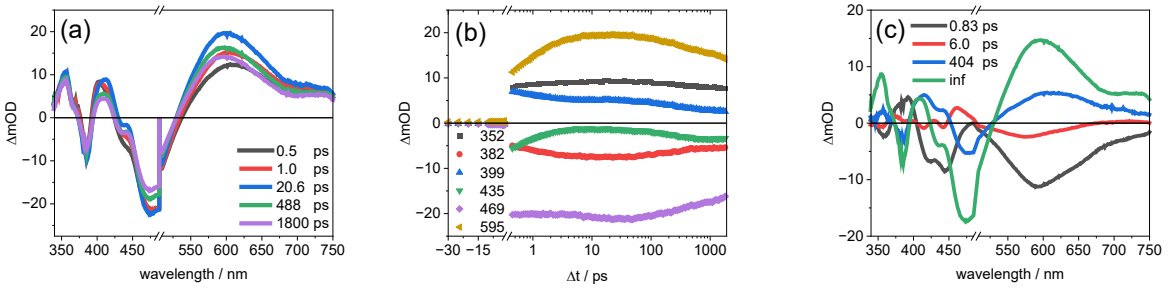

Figure S6: Chirp-corrected raw transient spectra (a), chirp-corrected raw kinetic traces (b) and decay associated spectra received from global fitting of RutpphzRhCp* dissolved in ACN, measured at room temperature in a standard 1 mm cuvette without the addition of further compounds.

After addition of TBACl

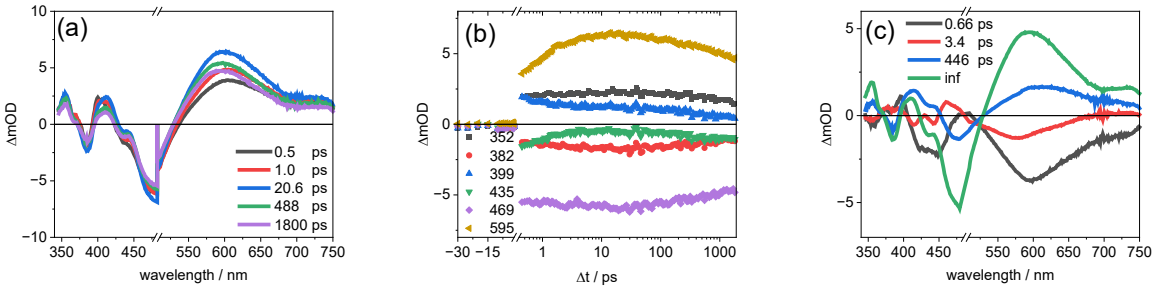

Figure S7: Chirp-corrected raw transient spectra (a), chirp-corrected raw kinetic traces (b) and decay associated spectra received from global fitting of RutpphzRhCp* dissolved in ACN, measured at room temperature in a standard 1 mm cuvette after adding 3.9 mM TBACl.

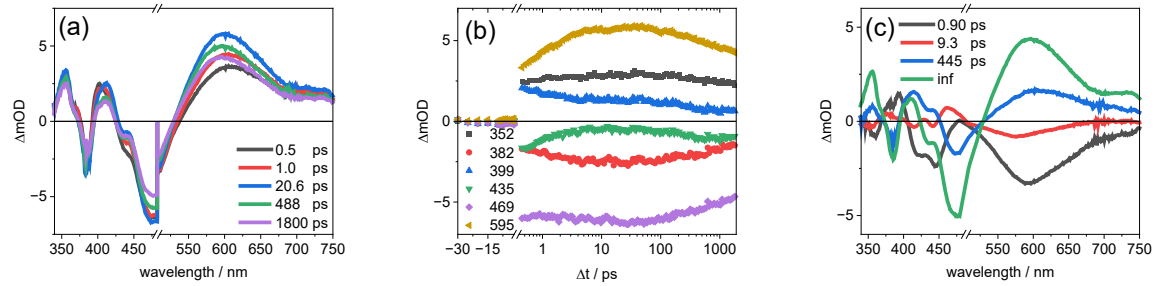

Figure S8: Chirp-corrected raw transient spectra (a), chirp-corrected raw kinetic traces (b) and decay associated spectra received from global fitting of RutpphzRhCp* dissolved in ACN, measured at room temperature in a standard 1 mm cuvette after adding 12 mM TBACl.

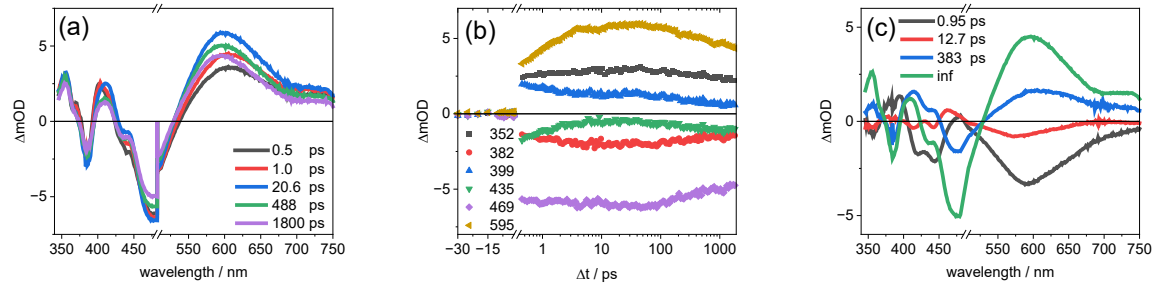

Figure S9: Chirp-corrected raw transient spectra (a), chirp-corrected raw kinetic traces (b) and decay associated spectra received from global fitting of RutpphzRhCp* dissolved in ACN, measured at room temperature in a standard 1 mm cuvette after adding 27 mM TBACl.

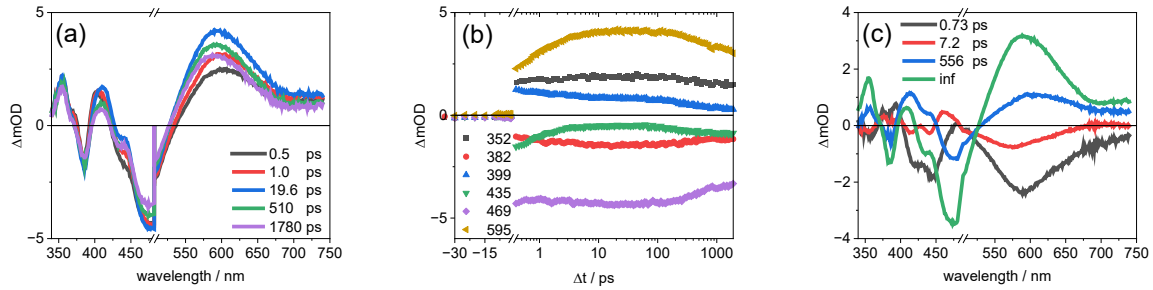

Figure S10: Chirp-corrected raw transient spectra (a), chirp-corrected raw kinetic traces (b) and decay associated spectra received from global fitting of RutpphzRhCp* dissolved in ACN, measured at room temperature in a standard 1 mm cuvette after adding 150 mM TBACl.

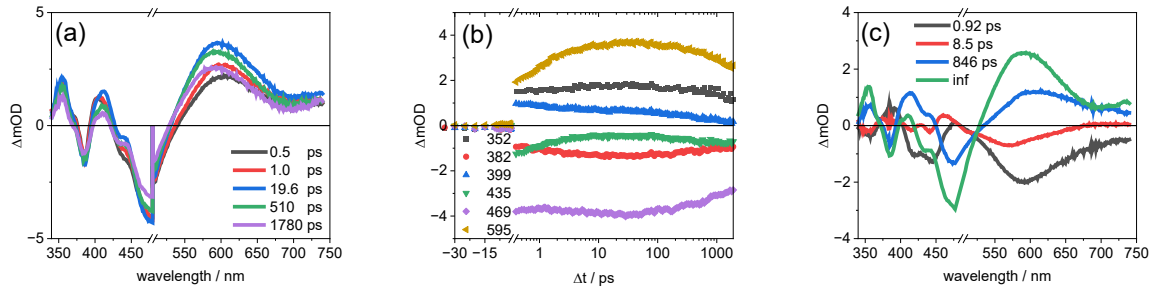

Figure S11: Chirp-corrected raw transient spectra (a), chirp-corrected raw kinetic traces (b) and decay associated spectra received from global fitting of RutpphzRhCp* dissolved in ACN, measured at room temperature in a standard 1 mm cuvette after adding 300 mM TBACl

After addition of $TBAPF_6$

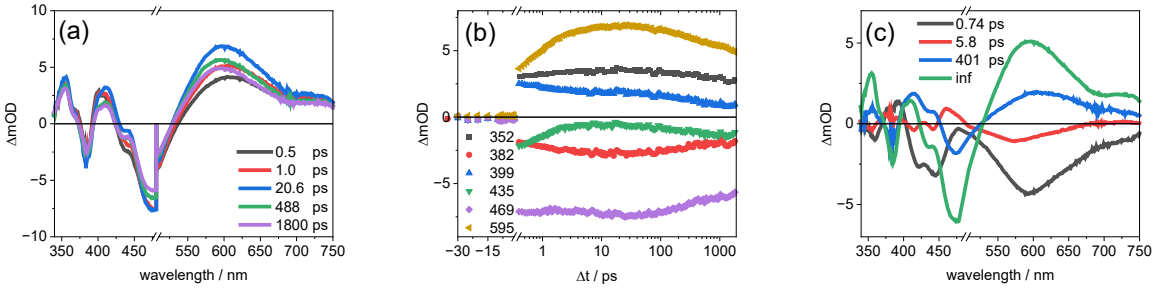

Figure S12: Chirp-corrected raw transient spectra (a), chirp-corrected raw kinetic traces (b) and decay associated spectra received from global fitting of RutpphzRhCp* dissolved in ACN, measured at room temperature in a standard 1 mm cuvette after adding 3 mM $TBAPF_6$

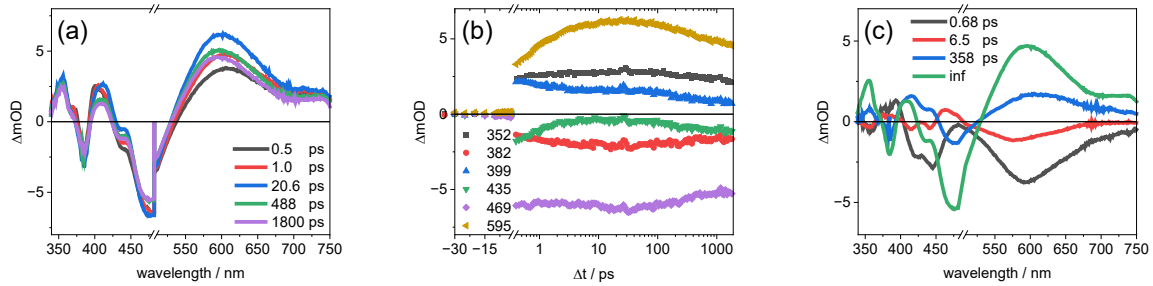

Figure S13: Chirp-corrected raw transient spectra (a), chirp-corrected raw kinetic traces (b) and decay associated spectra received from global fitting of RutpphzRhCp* dissolved in ACN, measured at room temperature in a standard 1 mm cuvette after adding 12.6 mM $TBAPF_6$

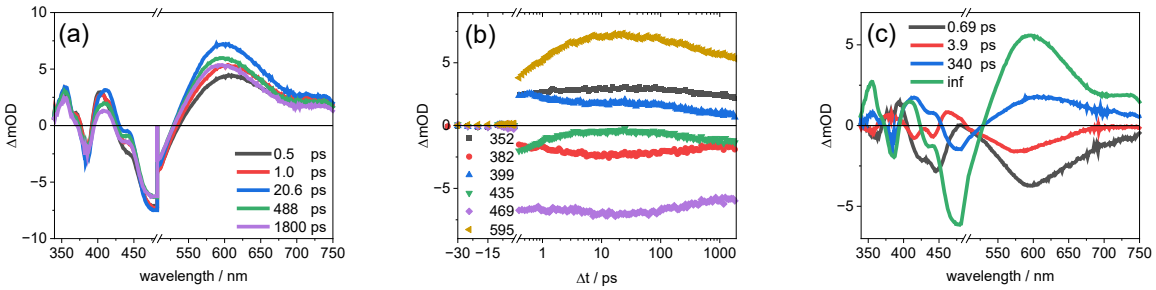

Figure S14: Chirp-corrected raw transient spectra (a), chirp-corrected raw kinetic traces (b) and decay associated spectra received from global fitting of RutpphzRhCp* dissolved in ACN, measured at room temperature in a standard 1 mm cuvette after adding 34.8 mM $TBAPF_6$

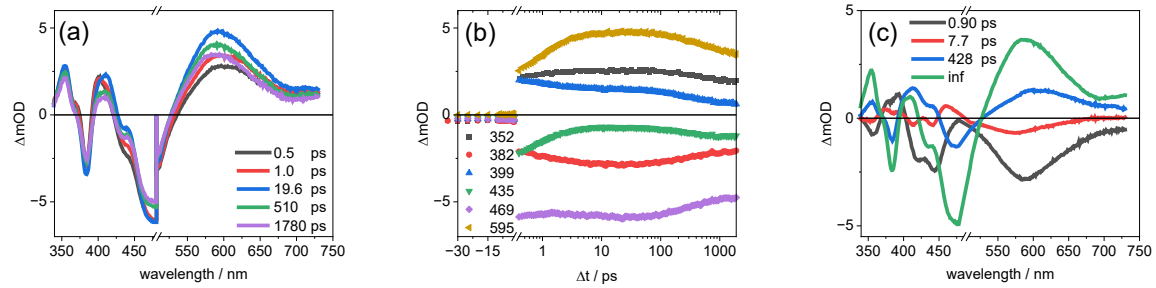

Figure S15: Chirp-corrected raw transient spectra (a), chirp-corrected raw kinetic traces (b) and decay associated spectra received from global fitting of RutpphzRhCp* dissolved in ACN, measured at room temperature in a standard 1 mm cuvette after adding 150 mM $TBAPF_6$

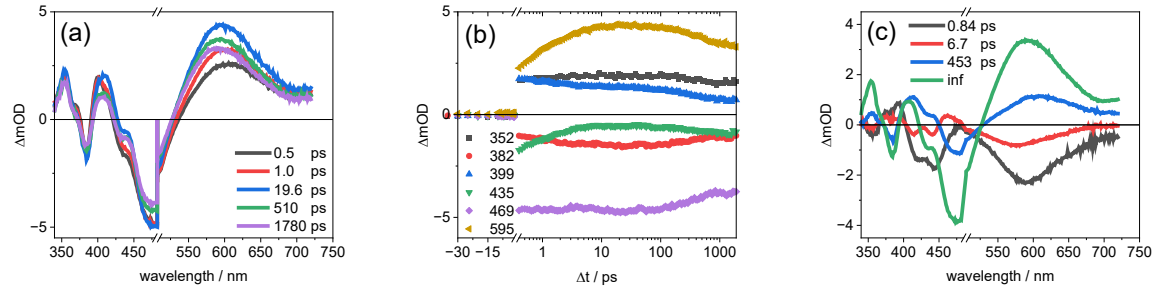

Figure S16: Chirp-corrected raw transient spectra (a), chirp-corrected raw kinetic traces (b) and decay associated spectra received from global fitting of RutpphzRhCp* dissolved in ACN, measured at room temperature in a standard 1 mm cuvette after adding 300 mM $TBAPF_6$

Effect of the added TBA-salts to the fitting results of the first two processes

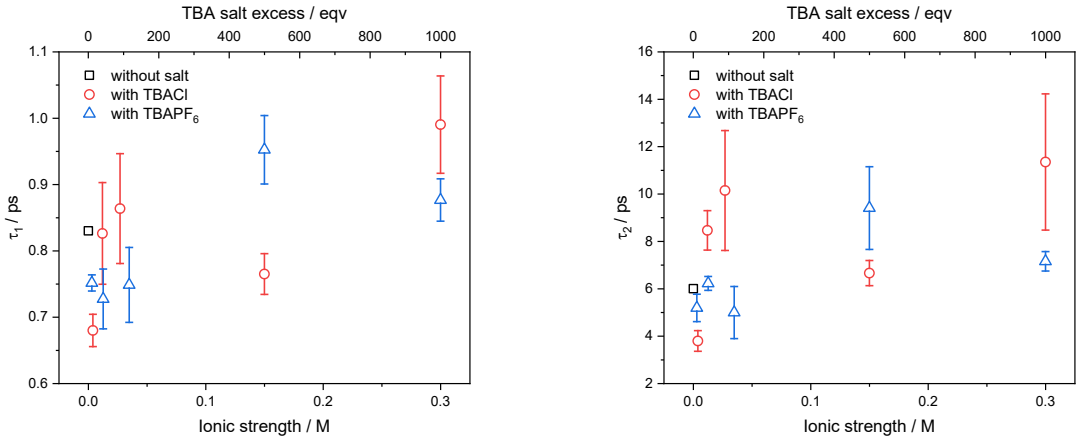

Figure 17: Time constants received from global fit vs. the ionic strength to the solution. Left τ_1, right τ_2.

References

1 B. Baumgartner, V. Glembockyte, A. J. Gonzalez-Hernandez, A. Valavalkar, R. J. Mayer, L. L. Fillbrook, A. Müller-Deku, J. Zhang, F. Steiner, C. Gross, M. Reynders, H. Munguba, A. Arefin, A. Ofial, J. E. Beves, T. Lohmueller, B. Dietzek-Ivanšic, J. Broichhagen, P. Tinnefeld, J. Levitz and O. Thorn-Seshold, *A general method for near-infrared photoswitching in biology, demonstrated by the >700 nm photocontrol of GPCR activity in brain slices*, 2024.

2 C. Müller, T. Pascher, A. Eriksson, P. Chabera and J. Uhlig, *J. Phys. Chem. A*, 2022, **126**, 4087–4099.

3 L. Zedler, A. K. Mengele, K. M. Ziems, Y. Zhang, M. Wächtler, S. Gräfe, T. Pascher, S. Rau, S. Kupfer and B. Dietzek, *Angew. Chem., Int. Ed.*, 2019, **58**, 13140-13148.